

[Click here to view linked References](#)

***In silico* analysis of the effects of disease-associated mutations of β -Hexosaminidase A in Tay-Sachs disease**

Mohammad Ihsan Fazal¹, Rafal Kacprzyk² and David J. Timson^{3*}

¹Brighton and Sussex Medical School, University of Sussex, Falmer, Brighton BN1 9PX. UK.

² School of Biological Sciences, Queen's University Belfast, Medical Biology Centre, 97 Lisburn Road, Belfast, BT9 7BL. UK.

³ School of Pharmacy and Biomolecular Sciences, University of Brighton, Huxley Building, Lewes Road, Brighton BN2 4GJ. UK.

* Corresponding author:

Address: School of Pharmacy and Biomolecular Sciences, University of Brighton, Huxley Building, Lewes Road, Brighton BN2 4GJ. UK.

Telephone +44(0)1273 641623

Email d.timson@brighton.ac.uk

Short title: *In silico* analysis of β -Hexosaminidase A

Category: Research article

Abstract

1 Tay-Sachs disease (TSD), a deficiency of β -Hexosaminidase A (Hex A), is a rare but debilitating
2 hereditary metabolic disorder. Symptoms include extensive neurodegeneration and often result in
3 death in infancy. We report an *in silico* study of 42 Hex A variants associated with the disease. Variants
4 were separated into three groups according to age of onset: infantile (n=28), juvenile (n=9) and adult
5 (n=5). Protein stability, aggregation potential and the degree of conservation of residues were
6 predicted using a range of *in silico* tools. We explored the relationship between these properties and
7 the age of onset of TSD. There was no significant relationship between protein stability and disease
8 severity or between protein aggregation and disease severity. Infantile TSD had a significantly higher
9 mean conservation score than non-disease associated variants. This was not seen in either juvenile or
10 adult TSD. This study has established that the degree of residue conservation may be predictive of
11 infantile TSD. It is possible these more highly conserved residues are involved in trafficking of the
12 protein to the lysosome. In addition, we developed and validated software tools to automate the
13 process of *in silico* analysis of proteins involved in inherited metabolic diseases. Further work is
14 required to identify the function of well-conserved residues to establish an *in silico* predictive model
15 of TSD severity.

16
17
18
19
20
21
22
23
24
25
26
27
28
29
30
31
32
33
34
35
36
37 **Keywords:** GM2 gangliosidosis; Sphingolipidosis; inherited metabolic disease; HexA; protein stability
38
39
40
41
42
43
44
45
46
47
48
49
50
51
52
53
54
55
56
57
58
59
60
61
62
63
64
65

Introduction

1
2 Tay-Sachs disease (TSD; Type I G_{M2} -gangliosidosis; OMIM#272800) is a rare, progressive autosomal
3
4 recessive disease with an incidence of one in 320,000 births in the general populations and a carrier
5
6 frequency of 1 in 250 (Lew *et al.*, 2015). Commonly fatal, it is caused by the abnormal metabolism of
7
8 GM1 ganglioside, a molecule that accounts for 10-12% of the total lipid content of neuronal cellular
9
10 membranes and contributes to approximately 1.5% of dry brain weight (Svennerholm & Fredman,
11
12 1980; Tettamanti, 2004). In healthy individuals, degradation of GM1 ganglioside occurs in the acidic
13
14 confines of the lysosome (Mark *et al.*, 2003). Subunits are removed sequentially from the ganglioside
15
16 with each step being catalysed by specific enzymes (Figure 1a). The conversion of GM2 to GM3 is
17
18 catalysed by β -Hexosaminidase A (HexA/EC 3.2.1.52), a heterodimeric enzyme composed of two
19
20 subunits, α and β , encoded by the genes *HexA* and *HexB* respectively (Henrissat & Davies, 1997). The
21
22 α -subunit is uniquely able to bind the negatively charged GM2 ganglioside/activator protein complex
23
24 and hydrolyse the terminal *N*-acetylgalactosamine (GalNAc) (Mark *et al.*, 2003; Sharma *et al.*, 2003a).
25
26 If a mutation in *HexA* causes HexA to dysfunction, GM2 accumulates within the neuron resulting in
27
28 TSD.
29
30
31
32
33
34
35

36 The human enzyme is a heterodimer of one α - and one β -subunit encoded by the *HEXA* and *HEXB*
37
38 genes respectively, β -Hexosaminidase A (Korneluk *et al.*, 1986; Neote *et al.*, 1988). Two other isoforms
39
40 of the β -hexosaminidase protein are present in humans – an $\alpha\alpha$ homodimer (β -hexosaminidase S) and
41
42 a $\beta\beta$ homodimer (β -hexosaminidase B) (Aruna & Basu, 1976; Hayase & Kritchevsky, 1973; Hepbilkler
43
44 *et al.*, 2002; Ikonne *et al.*, 1975; Robinson & Stirling, 1968). Structurally the α - and β -subunits have a
45
46 similar overall fold (root mean square deviation of approximately 0.7 Å over approximately 460
47
48 equivalent C_{α} atoms) (Lemieux *et al.*, 2006b). Both subunits contain an active site which catalyses the
49
50 hydrolysis of terminal *N*-acetylgalactosamine and *N*-acetylglucosamine residues from complex
51
52 polysaccharide moieties. The catalytic mechanism is postulated to involve two residues – Glu-323
53
54 which acts as a base and protonates the glycosidic oxygen atom and Asp-322 which acts as a base,
55
56 polarising the carbonyl in the *N*-acetyl group and stabilising the transition state (Lemieux *et al.*, 2006b;
57
58
59
60
61
62
63
64
65

1 Passos *et al.*, 2011). However, only the α -subunit can catalyse the hydrolysis of polysaccharides
2 containing sialic acid groups (Kytzia & Sandhoff, 1985). This specificity arises from different active site
3 structures: the α -subunit has a positively charged arginine residue which is able to bind to the
4 negatively charged sialic acid (Lemieux *et al.*, 2006b; Mark *et al.*, 2001; Sharma *et al.*, 2003b).
5
6

7
8
9 TSD occurs in four forms: infantile, juvenile, adult and the B1 variant. In infantile TSD, the most severe
10 form, patients appear normal until, within the first 6 months of life, there is developmental
11 retardation, muscular weakness and an increased startle response. As the disease progresses, there is
12 a loss of hearing and vision, cognitive impairment, seizures and paralysis resulting in death between 3
13 and 5 years of age (Fernandes Filho & Shapiro, 2004; Maegawa *et al.*, 2006b; Masingue *et al.*, 2020).
14
15

16
17 In juvenile TSD, onset occurs in childhood with one cohort study of 21 patients stating a mean onset
18 time of 5.3 ± 4.1 years with symptoms such as gait disturbances, ataxia, dysarthria and developmental
19 delay with a median survival time of 14.5 years (Maegawa *et al.*, 2006b). As the disease progresses
20 cognitive and motor skills deteriorate and anarthria, muscle wasting and incontinence occurs
21 (Maegawa *et al.*, 2006a; Specola *et al.*, 1990). Adult TSD has the most variable time of onset and is the
22 least severe of the three as it is not **always** fatal (Masingue *et al.*, 2020). One case series of 21 patients
23 reported a mean onset age of 18.1 years (Neudorfer *et al.*, 2005), whereas another study reported
24 onsets of 15 and 20 years (Hurowitz *et al.*, 1993). A separate case report reported onset age of 47 years
25 (Steiner *et al.*, 2016). Symptoms involve psychiatric disturbance, dysarthria, gait abnormalities, and leg
26 weakness. As the disease progresses the patient may require a wheelchair and experience dysphagia
27 and worsening of psychiatric state (Neudorfer *et al.*, 2005). The B1 variant can present as any of the
28 other variants. However, it exhibits a unique biochemical profile. HexA in B1 TSD is able to catalyse the
29 conversion of the neutral synthetic substrate 4-methylumbelliferyl-*N*-acetyl-fl-D-glucosamine, which is
30 sometimes used in diagnostic tests, but is unable to hydrolyse GM2 ganglioside *in vivo* or the acidic
31 synthetic substrate 4-methylumbelliferyl- β -D-*N*-acetylglucosamine-6-sulphate (Gordon *et al.*, 1988).
32
33 Although the neurological symptoms can be partially mitigated with drugs and other therapies, there
34 are no effective treatments available for Tay-Sachs disease. Potential treatments under development
35 include inhibition of substrate synthesis (thus reducing the accumulation of non-degraded G_{M2}
36
37
38
39
40
41
42
43
44
45
46
47
48
49
50
51
52
53
54
55
56
57
58
59
60
61
62
63
64
65

ganglioside), gene therapy, enzyme replacement therapy, neuronal stem cell transplants, pharmacological chaperones and gene editing (Akeboshi *et al.*, 2007; Cachon-Gonzalez *et al.*, 2006; Desnick & Kaback, 2001; Gray-Edwards *et al.*, 2018; Karumuthil-Melethil *et al.*, 2016; Kato *et al.*, 2017; Maegawa *et al.*, 2007; Ornaghi *et al.*, 2020; Ou *et al.*, 2020; Platt *et al.*, 2001; Rountree *et al.*, 2009; Tropak *et al.*, 2010; Tropak *et al.*, 2004; Tsuji *et al.*, 2011).

Here, we report an *in silico* investigation to explore how molecular changes in the HexA protein relate to the severity of TSD. The aim was to build the foundation for a predictive framework. Similar work has been done in the past to successfully develop predictive frameworks for several other diseases such as mevalonate kinase deficiency (Browne & Timson, 2015), type III galactosemia (McCorvie & Timson, 2013) and triose phosphate isomerase deficiency (Oliver & Timson, 2017). Developing a predictive framework that is reliable, accurate and effective could assist in the genetic counselling of a TSD carrier or in guiding prognoses for a TSD sufferer. As all studies were to be performed *in silico*, the opportunity arose to build software tools that could aid the accuracy and speed and reduce the cost of future work in this field.

Materials and Methods

Datasets

The identification of mutations known to be pathogenically associated with TSD was performed by a literature search using the NCBI PubMed database (<http://www.ncbi.nlm.nih.gov/PubMed>). Only mutations reported and categorised as pathogenic in the NCBI clinvar database were included (<http://www.ncbi.nlm.nih.gov/clinvar>). The classification of the disease was noted along with molecular consequence. Mutants were omitted if they resulted in early termination of the peptide, frameshift or were compound heterozygous. The crystal structure of wildtype human HexA (PDB: 2GJX) (Lemieux *et al.* 2006) was obtained from the Protein Data bank (<https://www.rcsb.org/>) (Berman *et*

1
2
3
4
5
6
7
8
9
10
11
12
13
14
15
16
17
18
19
20
21
22
23
24
25
26
27
28
29
30
31
32
33
34
35
36
37
38
39
40
41
42
43
44
45
46
47
48
49
50
51
52
53
54
55
56
57
58
59
60
61
62
63
64
65

al., 2000). The amino acid sequence of wildtype HexA was obtained from the UniProt database (<http://www.uniprot.org/uniprot/P06865>) (Pundir *et al.*, 2017; UniProt Consortium, 2018).

Structural analysis

YASARA (<http://www.yasara.org>) (Krieger *et al.*, 2009) is based on the AMBER force-field. It computationally solvates and energy minimises protein structures. All PDB files were processed through YASARA. Where possible, these energy-minimised structures were used for any analysis involving protein structure. Superpose (<http://wishart.biology.ualberta.ca/superpose/>) (Maiti *et al.*, 2004) calculates protein structure superpositions of two or more PDB files based on a modified quaternion eigenvalue approach. Comparisons were made between the wildtype PDB and each mutant variant PDB in turn, the root-mean-square deviation (RMSD) was recorded.

Prediction of biochemical effects of each missense mutation on HexA aggregation

Predicting the effect of a mutation on the aggregation propensity of the protein was done by using freely available software. Fluorescence probe measurement of live macrophages has shown intralysosomal pH to be 4.7 to 4.8 with other studies placing estimates between 4.5 and 5 (Coen *et al.*, 2012; Lange *et al.*, 2006; Ohkuma & Poole, 1978; Tabeta *et al.*, 2006). With this in mind, a pH of 5 was selected as the webserver only accepted pH as an integer. Additionally, a temperature of 310 K and an ionic strength of 0.15 M were used to replicate the human lysosomal conditions as best as the software allowed. All HexA sequences had the first 22 residues removed to simulate the initial proteolytic cleavage that occurs in the endoplasmic reticulum before HexA is trafficked to the lysosome (Little *et al.*, 1988).

TANGO (<http://tango.crg.es/>) uses a statistical mechanics algorithm to estimate the propensity for a protein to aggregate (Fernandez-Escamilla *et al.*, 2004). The C- and N-terminus status was set to free.

Zyggregator (<http://www-mvsoftware.ch.cam.ac.uk/index.php/zyggregator>) is a web server that uses the Zyggregator algorithm to make predictions of the propensity of polypeptide chains to form protofibrillar assemblies (Tartaglia & Vendruscolo, 2008). CamSol (<http://www-mvsoftware.ch.cam.ac.uk/index.php/camsolintrinsic>) is a web server that predicts the solubility and the generic aggregation propensity of a protein from a given sequence (Sormanni *et al.*, 2015).

Prediction of biochemical effects of each missense mutation on HexA stability and structure

Prediction of the effect of mutations on the stability of the protein was done by using several freely available web servers. I-Mutant 3.0 (<http://gpcr2.biocomp.unibo.it/cgi/predictors/I-Mutant3.0/I-Mutant3.0.cgi>) predicts the effect of a mutation on the stability of a protein (Capriotti *et al.*, 2008). It performs a requested point mutation on a provided PDB file or a single letter code amino acid sequence and returns the change in the Gibbs free energy change of unfolding compared to the wildtype protein ($\Delta\Delta G$). The wildtype HexA PDB file was used as an input and a pH of 5 and a temperature of 37 °C were chosen to replicate human lysosomal conditions. The Cologne University protein stability analysis tool (CUPSAT) available from (<http://cupsat.tu-bs.de/>) predicts the effects of point mutations on the overall protein stability. It returns the $\Delta\Delta G$ for every possible point mutation at a requested location using a PDB file (Parthiban *et al.*, 2006). The SDM server (<http://131.111.43.103/>) uses a knowledge-based system to predict the effect of a given list of mutations on a wildtype PDB file and returns the $\Delta\Delta G$ (Pandurangan *et al.*, 2017). The mutation Cutoff Scanning Matrix (mCSM) (<http://biosig.unimelb.edu.au/mcsm/stability>) (Pires *et al.*, 2014) uses predictive models trained with graph-based signatures to predict the effects of a given list of point mutations on the stability of a wildtype PDB file and returns the $\Delta\Delta G$.

Multiple sequence alignment and comparison of residue conservation of HexA variants

1 Wildtype HexA amino acid sequences were obtained from the NCBI protein database
2 (<http://www.ncbi.nlm.nih.gov/protein>). Only complete sequences of HexA found in the refSeq
3 database were included. A total of 101 sequences were identified including 79 mammals, 14 fish, five
4 birds, one lizard, one nematode and one plant. After elimination of duplicates, 73 homologous
5 sequences remained (for a full list, see Supplementary Table S1). These were input to a multiple
6 sequence alignment server Clustal Omega (<https://www.ebi.ac.uk/Tools/msa/clustalo/>) (Sievers *et al.*,
7 2011) with human HexA added to the first position. The resultant multiple aligned sequence was
8 entered into the Scorecons server to output Valdar conservation scores, an estimate of a residue's
9 conservation throughout multiple sequences (Valdar, 2002).
10
11
12
13
14
15
16
17
18
19
20
21
22
23

24 *Development of software tools to simplify and increase accuracy of data acquisition*

25
26
27 Python scripts were created using PyCharm (JetBrains, 2017) with manipulation of protein structures
28 (PDB files) performed by communicating with PyMol (Schrödinger, 2018) via its Application
29 Programming Interface (API). The openpyxl module (Gazoni, 2018) was used to read/write Microsoft
30 Excel files (ISO/IEC 29500-1:2016) in python. A python script loaded the energy minimised wildtype
31 HexA structure and a Microsoft Excel File containing a list of mutations stored as comma-separated
32 values (e.g. Arg,252,His). The comma-separated values were split and input sequentially to the
33 mutagenesis function within PyMol to produce PDB files for all mutants.
34
35
36
37
38
39
40
41
42
43
44

45 A command line based program was written in Pascal using Lazarus (Team, 2018) to facilitate the
46 production of mutant sequences and to output them as text files formatted for further analysis. The
47 program held a copy of the wildtype HexA sequence in memory. The user selects a residue and mutates
48 it to an amino acid single letter code of choice and saves it to a text file – the sequence is reset to
49 wildtype after every save. The program also allows for deletions, early terminations and can output
50 the length of the current sequence. A batch file was created in Notepad++ (Ho, 2018) (Ho, 2018) on
51
52
53
54
55
56
57
58
59
60
61
62
63
64
65

1 which the user can drag and drop text files to input it directly into TANGO thereby bypassing any
2 command line interaction.
3

4 R scripts were created using RStudio (Team, 2016). The RSelenium package (Harrison, 2017) was used
5 to automate interaction with and to extract data from webservers. The xlsx package (Dragulescu, 2014)
6 was used to read/write Microsoft Excel files in R. An R script was created to automate user interaction
7 with the Zyggregator web server. The script holds a copy of the wildtype HexA sequence in memory
8 and loads a Microsoft Excel file containing a list of mutations stored as comma-separated values. The
9 comma-separated values were split to yield the position of the mutation and the amino acid to mutate
10 to. The amino acids were converted from three letter code to single letter code (i.e. Arg to R) and the
11 wildtype HexA sequence was modified accordingly before being input to Zyggregator along with the
12 experimental conditions. The script is able to identify when the Zyggregator calculation is complete
13 and navigate to the results page. The relevant data is captured and stored in memory before being
14 saved to a Microsoft excel file. An identical approach was used to create an R script for CamSoli.
15
16
17
18
19
20
21
22
23
24
25
26
27
28
29
30

31 An R script was created to automate the user interaction of iMutant 3.0. The script contains the file
32 path to the energy minimised wildtype HexA structure and loads a comma separated values file (CSV)
33 containing a list of mutations. The comma-separated values are split to yield the location of mutation
34 and desired amino acid. The wildtype HexA structure is uploaded to iMutant 3.0 and experimental
35 conditions are entered. The script waits for iMutant 3.0 to finish its calculations before extracting the
36 $\Delta\Delta G$ values. An identical approach was used to create an R script for CUPSAT. An R script was also
37 created to automate the user interaction of Superpose. An approach similar to the iMutant 3.0 script
38 was taken. However, key differences were the need to upload both the wildtype and mutant PDB
39 rather than entering mutant locations and amino acids.
40
41
42
43
44
45
46
47
48
49
50
51
52
53

54 An important step in the automation of webservers was the identification of the desired result.
55 Superpose was the only webserver that consistently presented the result in the same cell of an html
56 table. In this case, it was straightforward to use RSelenium's getElementText request. The other
57 webservers presented the result in either plain text (Zyggregator, Camsoli, Imutant 3.0) or as a table
58
59
60
61
62
63
64
65

1 where the result could be in any row (CUPSAT). In this case a pattern recognition method (R-Project,
2 2018) was used to identify text containing the desired result. (For the patterns used, see supplements
3 E-H under the code comment “#Define patterns”.) All code was run with test data and samples of the
4
5 final outputs were manually examined to assess the level of function of the software tools.
6
7
8
9

10 11 12 *Data analysis*

13
14
15 All data analysis and graph production was carried out using Graphpad Prism.(GraphPad Software Inc.,
16 2017) Where data normalisation was performed, the equation $x_{new} = x_n/x_{wildtype}$ was used to
17
18 normalise data with respect to the wildtype. Where no wildtype value was available, the equation
19
20 $x_{new} = (x_n - x_{min})/(x_{max}-x_{min})$ was used to normalise the data with respect to the maximum and
21
22 minimum value. One-way ANOVA was used to assess whether there was any statistically significant
23
24 difference between the means of groups. Tukey post-hoc tests were done to identify which groups
25
26 were significantly different to each other. All graphs were plotted as the mean \pm standard deviation.
27
28
29
30
31
32
33 The significance threshold was set at $p < 0.05$.
34
35
36
37
38
39

40 **Results**

41 42 43 *Identification of point mutations pathogenic for Tay-Sachs Disease*

44
45
46 A total of 42 pathogenic variants were identified and included in this study. Of these, five exhibited an
47
48 adult TSD phenotype, 27 exhibited an infantile TSD phenotype and six exhibited a juvenile phenotype.
49
50
51 Additionally, two B1 variants exhibited an infantile phenotype and were included in the infantile group
52
53 and two B1 variants exhibited a juvenile phenotype and were included with this group. Table 1 outlines
54
55 the details of the variants identified. Infantile mutants were regarded as the most severe form, adult
56
57 the least severe and juvenile as intermediate. The positions of the residues affected were mapped
58
59
60
61
62
63
64
65

1 onto the HexA crystal structure (Figure 1b). These positions were located throughout the structure
2 and did not appear to cluster in any specific region.
3
4
5
6

7 *Effect of point mutations on aggregation potential*

8
9

10 The results from three aggregation calculators (Zygggregator, Camsoli and TANGO) were normalised
11 with respect to the wildtype. A mean aggregation score for each variant was then calculated. The
12 mean for each phenotype was then calculated and the results plotted in Figure 2a along with the
13 wildtype. There was no significant difference between any of the groups.
14
15
16
17
18
19
20
21
22
23

24 *Effect of point mutations on protein stability and structure*

25
26

27 The $\Delta\Delta G$ for all variants were obtained from four webserver (iMutant 3.0, CUPSAT, SDM, mCSM) and
28 normalised with respect to the minimum and maximum values. The mean $\Delta\Delta G$ for each variant was
29 calculated and an overall mean for each phenotype was plotted in Figure 2b. There was no significant
30 difference in mean $\Delta\Delta G$ between groups. The root mean square deviation (RMSD) for the energy
31 minimised model of each variant compared to wildtype was calculated using the Superpose webserver.
32 Mean RMSD was calculated for each phenotype and plotted in Figure 2c. There was no significant
33 difference in mean RMSD between the groups.
34
35
36
37
38
39
40
41
42
43
44
45
46
47

48 *Degree of conservation of residues affected by mutations*

49
50

51 The mean conservation scores of non-disease associated residues were compared to the mean
52 conservation scores of each phenotype and plotted in Figure 2d. There was a highly significant
53 difference ($p=0.001$) in mean conservation scores between the non-disease associated residues and
54 the infantile phenotype residues. There were no significant differences seen with the adult or juvenile
55 groups.
56
57
58
59
60
61
62
63
64
65

Software tools to simplify and increase accuracy of data acquisition

A number of tools were created to help automate these analyses (and similar analyses for other diseases). These tools have been made publicly available at the Open Science Framework (www.osf.io/a5gsb) and examples of their implementation are shown in Figure 3. A python script was created to automate the production of variant PDB files. This enabled the automated generation of (unminimised) variant models of the protein in pdb file format from an Excel file containing details of the variants (Figure 3a). To automate analysis using the TANGO webserver, a pascal command line program was created along with a system to enable operation via a batch file (Figure 3b, c). R-scripts were generated to automate the use of Zyggregator (Figure 3d), Camsoli (Supplementary Figure S1a), iMutant 3.0 (Supplementary Figure S1b), CUPSAT (Supplementary Figure S1c) and Superpose (Supplementary Figure S1d).

Discussion

The 45 variants that were included in this study represent all point mutations known to be pathogenic for TSD. The separation of the variants into each phenotype and the placement of the phenotypes on a spectrum from severe to least severe is appropriate when considering the description of each clinical case (see Table 1). The exclusion criteria omitted those mutations where the cause of reduced HexA activity is obvious and where the approach adopted in this paper would not be appropriate. For example, the most common infantile TSD mutation is a 4bp insertion causing a frame-shift and early termination resulting in a protein considerably different to wildtype (Boles & Proia, 1995).

The webservers and software used in this project, are manageable when used individually or for small numbers of variants. However, when used in combination the manual entry of data becomes a time-consuming and error prone process. A study using 195 computer literate participants, found that manually entering data and visually checking it against the source resulted in an error rate nearly three

times as high as when using computer assisted double entry data validation (Barchard & Pace, 2011).

1 Given the multiple entry of data was not an option here, the automation of data entry proved an
2 attractive alternative. The scripts and software we have developed have been shown to work correctly.
3
4

5
6 Some HexA mutants have been reported to have a propensity to aggregate (Dersh *et al.*, 2016; Proia
7 & Neufeld, 1982) and it has been shown that aggregation plays a role in other metabolic
8 disorders.(Bang *et al.*, 2009; McCorvie & Timson, 2013) Considering this, we explored whether
9 aggregation plays a role in determining TSD severity. After comparing the mean aggregation scores,
10 there were no significant differences in predicted aggregation between the TSD phenotypes or
11 wildtype, suggesting that in any form of TSD, HexA is no more likely to aggregate than wildtype and so
12 the loss of HexA function lies elsewhere.
13
14
15
16
17
18
19
20
21

22
23 $\Delta\Delta G$ is a useful indicator of protein stability, the higher it is the less stable the mutant protein compared
24 to the wildtype (Funahashi *et al.*, 2003). Some webserver predicted much larger $\Delta\Delta G$ values than
25 others did, for example, Lys197Thr was predicted to have a $\Delta\Delta G$ of -0.94 kcal/mol by iMutant 3.0 but
26 -11.01 kcal/mol by CUPSAT. Considering this, it was necessary to normalise the data with respect to
27 the minimum and maximum values to make it easier to draw comparisons from each server. It is
28 important to note that in doing this we assumed that the servers are equally accurate. From calculating
29 the mean $\Delta\Delta G$ from all four servers and comparing the mean $\Delta\Delta G$ of each phenotype, there was no
30 significant difference between any groups. This suggests that changes in enzyme stability are not
31 responsible for the increased loss of HexA function seen in more severe TSD.
32
33
34
35
36
37
38
39
40
41
42
43
44
45

46 Conservation analysis relies on the principle that in homologous proteins, residues that are more
47 conserved throughout different organisms play a more important role in the function of the enzyme.
48
49

50 It has been used to identify functionally important residues in protein interaction interfaces (Mintseris
51 & Weng, 2005), ligand-binding sites (Liang *et al.*, 2006) and in maintaining overall protein structure
52 (Valdar & Thornton, 2001). In this study, we carried out a multiple protein sequence alignment of
53 human HexA with the enzyme from 73 other species. By comparing the mean Valdar conservation
54 score of disease-associated residues, there was no significant difference between TSD phenotypes.
55
56
57
58
59
60
61
62
63
64
65

1 However, when residues associated with TSD phenotypes were compared with non-disease associated
2 residues there was a highly significant difference in conservation ($p=0.001$) between infantile TSD and
3 the non-disease associated residues. Infantile TSD had a greater mean conservation score than
4 wildtype (0.8425 ± 0.1564 vs 0.6635 ± 0.2517). This suggests that the location of the mutation plays an
5 important role in determining the severe loss of HexA function in infantile TSD but not in the other
6 phenotypes.
7
8
9
10
11

12 Considering this in the context of the predictions of protein stability it is unlikely these conserved
13 residues play a role in maintaining stability. Mutations of the active site of HexA are regarded as rare,
14 only seen in the B1 variant (Lemieux *et al.*, 2006a; Ohno *et al.*, 2008). It is more likely that the affected
15 residues are involved in the trafficking of the protein into the lysosome or the interaction between the
16 α and β subunits. In fact, Dersh *et al.* observed that an infantile TSD variant, Glu482Lys, fails to associate
17 with the β subunit while an adult TSD variant, Gly269Ser, does so correctly (Dersh *et al.*, 2016). Lemieux
18 *et al.*, reiterate this and additionally state the variant is unable to exit the endoplasmic reticulum
19 (Lemieux *et al.*, 2006a). When the HEXB crystal structure was compared with HexA molecular models,
20 the interaction of the α and β subunit creates the docking site for the substrate/GM2 activator complex
21 so that a correct protein-protein interface here is critical for enzyme function (Mark *et al.*, 2003).
22 Immunoblotting using an anti- α subunit antibody in whole-cell lysates of HEK293T cells expressing
23 either wildtype, Glu482Lys (infantile TSD) and Gly269Ser (adult TSD) HexA showed that only the
24 wildtype was proteolytically cleaved to the final mature form suggesting either the variants were
25 unable to be cleaved or that they never reached the lysosome. Although these experiments focused
26 on only two variants, they demonstrate that several factors influence the severity of disease. HexA
27 leaving the endoplasmic reticulum, being trafficked to the lysosome, being cleaved correctly, correct
28 interaction between the α and β subunits and having an intact active site capable of interacting with
29 the substrate are all important considerations.
30
31
32
33
34
35
36
37
38
39
40
41
42
43
44
45
46
47
48
49
50
51
52
53
54
55

56 This *in silico* study has established that protein stability and aggregation potential of HexA variants do
57 not appear play significant roles in determining the severity of TSD. Residue conservation is
58
59
60
61
62
63
64
65

1 implicated in infantile TSD. It is possible these more highly conserved residues are involved in
2 trafficking of the protein to the lysosome but experimental studies are required to confirm this. It
3 appears that TSD has a different underlying molecular pathology compared to a number of other
4 inherited metabolic diseases. A recent study demonstrated that lysosomal proteins, like HexA, are
5 unusually thermally stable compared to those in other cellular compartments (Collier *et al.*, 2020).
6 This suggests that small changes in thermal stability are unlikely to have a significant effect on *in vivo*
7 function.
8
9

10
11
12
13
14
15
16 In several other cases, *in silico* studies have predicted that reduced protein stability is a key factor in
17 the loss of enzymatic activity (Timson, 2015). The majority of these studies concerned enzymes which
18 are synthesised and which function in the cellular cytoplasm. In contrast HexA is trafficked to the
19 lysosome, normally a much more acidic environment. This trafficking involves the recognition and
20 cleavage of a signal sequence. These events provide additional steps which are vulnerable to point
21 mutations and structural changes. This study suggests that these steps are the ones critically affected
22 by the majority of mutations associated with Tay-Sachs Disease.
23
24
25
26
27
28
29
30
31
32
33
34
35

36 **Acknowledgements**

37
38 **Funding:** RK was supported by a summer studentship funded by Queen's University, Belfast. This
39 research did not receive any other specific grant from funding agencies in the public, commercial, or
40 not-for-profit sectors.
41
42
43
44

45 **Declarations of interest:** The authors have none to declare.
46

47 **Data Availability:** Data will be available from the authors on request and will be placed in the
48 University of Brighton online repository: research.brighton.ac.uk
49
50
51
52
53
54
55
56
57
58
59
60
61
62
63
64
65

1
2
3
4
5
6
7
8
9
10
11
12
13
14
15
16
17
18
19
20
21
22
23
24
25
26
27
28
29
30
31
32
33
34
35
36
37
38
39
40
41
42
43
44
45
46
47
48
49
50
51
52
53
54
55
56
57
58
59
60
61
62
63
64
65

Figure legends

1
2 Figure 1: The pathway of GM1 ganglioside degradation and structure of β -Hexosaminidase A α subunit
3
4 (HexA). (a) Tay-Sachs Disease occurs when a mutated α subunit causes β -Hexosaminidase A to
5
6 dysfunction resulting in the accumulation of GM2 and eventual neuronal cell death. (b) The structure
7
8 of one monomer of the HexA protein with the location of residues known to be affected by disease-
9
10 mutations mapped. The backbone of the protein is shown in cartoon format in grey. Affected residues
11
12 are shown in stick format coloured red for those associated with the infantile onset form of the disease,
13
14 blue for those associated with the juvenile form and yellow for the adult form. A small number of
15
16 residues were associated with both the infantile and juvenile forms (purple), the infantile and adult
17
18 forms (orange) and the juvenile and adult forms (green). The images represent a single subunit from
19
20 the crystal structure of HexA (PDB: 2GJX) which had been subjected to energy minimisation. The lower
21
22 image related to the upper one by a rotation of 180° around the y-axis. The images were generated
23
24 using PyMol (www.pymol.org).
25
26
27
28
29
30

31 Figure 2: *In silico* analysis of HexA variants associated with Tay-Sachs Disease. (a) Mean and SD of
32
33 normalised aggregation potential of the three TSD phenotype groups and wildtype calculated from
34
35 three aggregation webservers (Zyggregator, Camsoli and TANGO). P-values obtained from Tukey
36
37 post hoc test. There was no significant difference in aggregation potential between the groups. (b)
38
39 Mean and SD of normalised $\Delta\Delta G$ of the three TSD phenotype groups calculated from four protein
40
41 stability web servers (iMutant 3.0, CUPSAT, SDM, mCSM). P-values obtained from Tukey post hoc
42
43 test. There was no significant difference in protein stability between the groups. (c) Mean and SD of
44
45 RMSD of the three TSD phenotype groups calculated from a RMSD web server (Superpose). P-values
46
47 obtained from Tukey post hoc test. There was no significant difference in protein RMSD between the
48
49 groups. (d) Figure 2 Mean and SD for conservation score for disease associated and non-disease
50
51 associated HexA residues calculated by the Scorecons server using a human HexA sequence aligned
52
53 with HexA sequences from 74 other species. There is a highly significant difference between no
54
55 disease and the severe infantile form.
56
57
58
59
60
61
62
63
64
65

Figure 3: Examples of the implementation of software tools developed in this study. (a) PDB file produced by python script for the mutant Arg252His visualised in PyMol. A command to select residue 252 has been executed (red box) to highlight position 252 in the single code sequence (red arrow). Residue 252 is Histamine rather than the wildtype Arginine demonstrating the mutation has taken place and the python script functions correctly. (b) Input (left) and output (right) of the pascal program for automating analysis by TANGO. A mutation at position 25 (correlating to position 3 after post-translational cleavage) has been carried out. Position 3 of the output is Histidine as expected and the sequence is preceded with the correct parameters for TANGO. (c) Dragging Test.txt onto the batch file (upper left) results in execution of TANGO analysis of the correct file (upper right) and as expected outputs an aggregation score in Test_Aggregation.txt (bottom) matching the output seen when running TANGO manually (not shown). (d) A test input of Arg,252,His (left) is correctly read and split by the R script. This displays variables in memory during execution of the code, note 'res' and 'mut' correctly correspond to the input (upper middle) and the file output from the script (right). The aggregation score is the same as that obtained from the input being entered manually (lower middle).

1
2
3
4
5
6
7
8
9
10
11
12
13
14
15
16
17
18
19
20
21
22
23
24
25
26
27
28
29
30
31
32
33
34
35
36
37
38
39
40
41
42
43
44
45
46
47
48
49
50
51
52
53
54
55
56
57
58
59
60
61
62
63
64
65

References

- 1
2 Ainsworth, P. J. Coulter-Mackie, M. B. (1992). A double mutation in exon 6 of the beta-
3 hexosaminidase alpha subunit in a patient with the B1 variant of Tay-Sachs disease. *Am J*
4 *Hum Genet* **51**, 802-9.
5
6 Akalin, N., Shi, H. P., Vavougiou, G., Hechtman, P., Lo, W., Scriver, C. R., *et al.* (1992). Novel Tay-
7 Sachs disease mutations from China. *Hum Mutat* **1**, 40-6.
8
9 Akeboshi, H., Chiba, Y., Kasahara, Y., Takashiba, M., Takaoka, Y., Ohsawa, M., *et al.* (2007).
10 Production of recombinant β -hexosaminidase A, a potential enzyme for replacement
11 therapy for Tay-Sachs and Sandhoff diseases, in the methylotrophic yeast *Ogataea minuta*.
12 *Applied and Environmental Microbiology* **73**, 4805-4812.
13
14 Akli, S., Chelly, J., Lacorte, J. M., Poenaru, L. & Kahn, A. (1991). Seven novel Tay-Sachs mutations
15 detected by chemical mismatch cleavage of PCR-amplified cDNA fragments. *Genomics* **11**,
16 124-34.
17
18 Akli, S., Chomel, J. C., Lacorte, J. M., Bachner, L., Kahn, A. & Poenaru, L. (1993a). Ten novel
19 mutations in the HEXA gene in non-Jewish Tay-Sachs patients. *Human molecular genetics* **2**,
20 61-67.
21
22 Akli, S., Chomel, J. C., Lacorte, J. M., Bachner, L., Kahn, A. & Poenaru, L. (1993b). Ten novel
23 mutations in the HEXA gene in non-Jewish Tay-Sachs patients. *Hum Mol Genet* **2**, 61-7.
24
25 Aruna, R. M. Basu, D. (1976). Purification and properties of β -hexosaminidase B from monkey brain.
26 *Journal of neurochemistry* **27**, 337-339.
27
28 Bang, Y. L., Nguyen, T. T., Trinh, T. T., Kim, Y. J., Song, J. & Song, Y. H. (2009). Functional analysis of
29 mutations in UDP-galactose-4-epimerase (GALE) associated with galactosemia in Korean
30 patients using mammalian GALE-null cells. *FEBS J* **276**, 1952-61.
31
32 Barchard, K. A. Pace, L. A. (2011). Preventing human error: The impact of data entry methods on
33 data accuracy and statistical results. *Computers in Human Behavior* **27**, 1834-1839.
34
35 Berman, H. M., Westbrook, J., Feng, Z., Gilliland, G., Bhat, T. N., Weissig, H., *et al.* (2000). The
36 Protein Data Bank. *Nucleic Acids Res* **28**, 235-42.
37
38 Boles, D. J. Proia, R. L. (1995). The molecular basis of HEXA mRNA deficiency caused by the most
39 common Tay-Sachs disease mutation. *Am J Hum Genet* **56**, 716-24.
40
41 Boonyawat, B. P., Tim; Nabangchang, Charcrin; Suwanpakdee, Piradee; (2016). A novel frameshift
42 mutation of HEXA gene in the first family with classical infantile Tay-Sachs disease in
43 Thailand. *Neurology Asia* **21**, 281-285.
44
45 Brown, C. A., Neote, K., Leung, A., Gravel, R. A. & Mahuran, D. J. (1989). Introduction of the alpha
46 subunit mutation associated with the B1 variant of Tay-Sachs disease into the beta subunit
47 produces a beta-hexosaminidase B without catalytic activity. *J Biol Chem* **264**, 21705-10.
48
49 Browne, C. Timson, D. J. (2015). *In Silico* Prediction of the Effects of Mutations in the Human
50 Mevalonate Kinase Gene: Towards a Predictive Framework for Mevalonate Kinase
51 Deficiency. *Ann Hum Genet* **79**, 451-9.
52
53 Cachon-Gonzalez, M. B., Wang, S. Z., Lynch, A., Ziegler, R., Cheng, S. H. & Cox, T. M. (2006).
54 Effective gene therapy in an authentic model of Tay-Sachs-related diseases. *Proceedings of*
55 *the National Academy of Sciences of the United States of America* **103**, 10373-10378.
56
57 Capriotti, E., Fariselli, P., Rossi, I. & Casadio, R. (2008). A three-state prediction of single point
58 mutations on protein stability changes. *BMC Bioinformatics* **9** Suppl 2, S6.
59
60 Coen, K., Flannagan, R. S., Baron, S., Carraro-Lacroix, L. R., Wang, D., Vermeire, W., *et al.* (2012).
61 Lysosomal calcium homeostasis defects, not proton pump defects, cause endo-lysosomal
62 dysfunction in PSEN-deficient cells. *J Cell Biol* **198**, 23-35.
63
64
65

- 1 Collier, A. M., Nemtsova, Y., Kuber, N., Banach-Petrosky, W., Modak, A., Sleat, D. E., *et al.* (2020).
2 Lysosomal protein thermal stability does not correlate with cellular half-life: global
3 observations and a case study of tripeptidyl-peptidase 1. *Biochem J* **477**, 727-745.
- 4 De Gasperi, R., Gama Sosa, M. A., Battistini, S., Yeretsian, J., Raghavan, S., Zelnik, N., *et al.* (1996).
5 Late-onset GM2 gangliosidosis: Ashkenazi Jewish family with an exon 5 mutation (Tyr180--
6 >His) in the Hex A alpha-chain gene. *Neurology* **47**, 547-52.
- 7 Dersh, D., Iwamoto, Y. & Argon, Y. (2016). Tay-Sachs disease mutations in HEXA target the alpha
8 chain of hexosaminidase A to endoplasmic reticulum-associated degradation. *Mol Biol Cell*
9 **27**, 3813-3827.
- 10 Desnick, R. J. Kaback, M. M. (2001). Future perspectives for Tay-Sachs disease. *Advances in Genetics*
11 **44**, 349-356.
- 12 Dragulescu, A. A. (2014). xlsx 0.5.7: Read, write, format Excel 2007 and Excel 97/2000/XP/2003 files.
- 13 Drucker, L., Hemli, J. A. & Navon, R. (1997). Two mutated HEXA alleles in a Druze patient with late-
14 infantile Tay-Sachs disease. *Hum Mutat* **10**, 451-7.
- 15 Drucker, L., Proia, R. L. & Navon, R. (1992). Identification and rapid detection of three Tay-Sachs
16 mutations in the Moroccan Jewish population. *Am J Hum Genet* **51**, 371-7.
- 17 Fernandes Filho, J. A. Shapiro, B. E. (2004). Tay-Sachs disease. *Arch Neurol* **61**, 1466-8.
- 18 Fernandes, M., Kaplan, F., Natowicz, M., Prence, E., Kolodny, E., Kaback, M., *et al.* (1992). A new
19 Tay-Sachs disease B1 allele in exon 7 in two compound heterozygotes each with a second
20 novel mutation. *Hum Mol Genet* **1**, 759-61.
- 21 Fernandes, M. J., Hechtman, P., Boulay, B. & Kaplan, F. (1997). A chronic GM2 gangliosidosis variant
22 with a HEXA splicing defect: quantitation of HEXA mRNAs in normal and mutant fibroblasts.
23 *Eur J Hum Genet* **5**, 129-36.
- 24 Fernandez-Escamilla, A. M., Rousseau, F., Schymkowitz, J. & Serrano, L. (2004). Prediction of
25 sequence-dependent and mutational effects on the aggregation of peptides and proteins.
26 *Nat Biotechnol* **22**, 1302-6.
- 27 Funahashi, J., Sugita, Y., Kitao, A. & Yutani, K. (2003). How can free energy component analysis
28 explain the difference in protein stability caused by amino acid substitutions? Effect of three
29 hydrophobic mutations at the 56th residue on the stability of human lysozyme. *Protein Eng*
30 **16**, 665-71.
- 31 Gazoni, E. C., C. (2018). Openpyxl 2.5.0 - A Python library to read/write Excel 2010 xlsx/xlsm files.
- 32 Giraud, C., Dussau, J., Azouguene, E., Feillet, F., Puech, J. P. & Caillaud, C. (2010). Rapid
33 identification of HEXA mutations in Tay-Sachs patients. *Biochem Biophys Res Commun* **392**,
34 599-602.
- 35 Gordon, B. A., Gordon, K. E., Hinton, G. G., Cadera, W., Feleki, V., Bayleran, J., *et al.* (1988). Tay-
36 Sachs disease: B1 variant. *Pediatr Neurol* **4**, 54-7.
- 37 GraphPad Software Inc. (2017). GraphPad Prism 7.04.
- 38 Gray-Edwards, H. L., Randle, A. N., Maitland, S. A., Benatti, H. R., Hubbard, S. M., Canning, P. F., *et*
39 *al.* (2018). Adeno-Associated Virus Gene Therapy in a Sheep Model of Tay-Sachs Disease.
40 *Hum Gene Ther* **29**, 312-326.
- 41 Harrison, J. (2017). R Selenium 1.71: R Bindings for 'Selenium WebDriver'.
- 42 Hayase, K. Kritchevsky, D. (1973). Separation and comparison of isoenzymes of *N*-acetyl- β -D-
43 hexosaminidase of pregnancy serum by polyacrylamide gel electrofocusing. *Clinica chimica*
44 *acta; international journal of clinical chemistry* **46**, 455-464.
- 45 Henrissat, B. Davies, G. (1997). Structural and sequence-based classification of glycoside hydrolases.
46 *Curr Opin Struct Biol* **7**, 637-44.

- 1 Hepbildikler, S. T., Sandhoff, R., Kolzer, M., Proia, R. L. & Sandhoff, K. (2002). Physiological
2 substrates for human lysosomal β -hexosaminidase S. *The Journal of biological chemistry* **277**,
3 2562-2572.
- 4 Ho, D. (2018). Notepad++ 7.5.5.
- 5 Hou, Y., Vavougiou, G., Hinek, A., Wu, K. K., Hechtman, P., Kaplan, F., *et al.* (1996). The Val192Leu
6 mutation in the alpha-subunit of beta-hexosaminidase A is not associated with the B1-
7 variant form of Tay-Sachs disease. *Am J Hum Genet* **59**, 52-8.
- 8 Hurowitz, G. I., Silver, J. M., Brin, M. F., Williams, D. T. & Johnson, W. G. (1993). Neuropsychiatric
9 aspects of adult-onset Tay-Sachs disease: two case reports with several new findings. *J*
10 *Neuropsychiatry Clin Neurosci* **5**, 30-6.
- 11 Ikonne, J. U., Rattazzi, M. C. & Desnick, R. J. (1975). Characterization of Hex S, the major residual β -
12 hexosaminidase activity in type O Gm2 gangliosidosis (Sandhoff-Jatzkewitz disease).
13 *American Journal of Human Genetics* **27**, 639-650.
- 14 JetBrains (2017). PyCharm.
- 15
16 Karumuthil-Meethil, S., Nagabhushan Kalburgi, S., Thompson, P., Tropak, M., Kaytor, M. D.,
17 Keimel, J. G., *et al.* (2016). Novel Vector Design and Hexosaminidase Variant Enabling Self-
18 Complementary Adeno-Associated Virus for the Treatment of Tay-Sachs Disease. *Hum*
19 *Gene Ther* **27**, 509-21.
- 20
21 Kato, A., Nakagome, I., Nakagawa, S., Kinami, K., Adachi, I., Jenkinson, S. F., *et al.* (2017). In silico
22 analyses of essential interactions of iminosugars with the Hex A active site and evaluation of
23 their pharmacological chaperone effects for Tay-Sachs disease. *Org Biomol Chem* **15**, 9297-
24 9304.
- 25
26 Kaufman, M., Grinshpun-Cohen, J., Karpati, M., Peleg, L., Goldman, B., Akstein, E., *et al.* (1997).
27 Tay-Sachs disease and HEXA mutations among Moroccan Jews. *Hum Mutat* **10**, 295-300.
- 28
29 Korneluk, R. G., Mahuran, D. J., Neote, K., Klavins, M. H., O'Dowd, B. F., Tropak, M., *et al.* (1986).
30 Isolation of cDNA clones coding for the α -subunit of human β -hexosaminidase. Extensive
31 homology between the α - and β -subunits and studies on Tay-Sachs disease. *The Journal of*
32 *biological chemistry* **261**, 8407-8413.
- 33
34 Krieger, E., Joo, K., Lee, J., Lee, J., Raman, S., Thompson, J., *et al.* (2009). Improving physical
35 realism, stereochemistry, and side-chain accuracy in homology modeling: Four approaches
36 that performed well in CASP8. *Proteins* **77 Suppl 9**, 114-122.
- 37
38 Kytzia, H. J. Sandhoff, K. (1985). Evidence for two different active sites on human β -hexosaminidase
39 A. Interaction of GM2 activator protein with β -hexosaminidase A. *The Journal of biological*
40 *chemistry* **260**, 7568-7572.
- 41
42 Lange, P. F., Wartosch, L., Jentsch, T. J. & Fuhrmann, J. C. (2006). CIC-7 requires Ostm1 as a beta-
43 subunit to support bone resorption and lysosomal function. *Nature* **440**, 220-3.
- 44
45 Lemieux, M. J., Mark, B. L., Cherney, M. M., Withers, S. G., Mahuran, D. J. & James, M. N. (2006a).
46 Crystallographic structure of human beta-hexosaminidase A: interpretation of Tay-Sachs
47 mutations and loss of GM2 ganglioside hydrolysis. *J Mol Biol* **359**, 913-29.
- 48
49 Lemieux, M. J., Mark, B. L., Cherney, M. M., Withers, S. G., Mahuran, D. J. & James, M. N. (2006b).
50 Crystallographic structure of human β -hexosaminidase A: interpretation of Tay-Sachs
51 mutations and loss of GM2 ganglioside hydrolysis. *Journal of Molecular Biology* **359**, 913-929.
- 52
53 Lew, R. M., Burnett, L., Proos, A. L. & Delatycki, M. B. (2015). Tay-Sachs disease: current
54 perspectives from Australia. *Appl Clin Genet* **8**, 19-25.
- 55
56 Liang, S., Zhang, C., Liu, S. & Zhou, Y. (2006). Protein binding site prediction using an empirical
57 scoring function. *Nucleic Acids Res* **34**, 3698-707.
- 58
59
60
61
62
63
64
65

- 1 Little, L. E., Lau, M. M., Quon, D. V., Fowler, A. V. & Neufeld, E. F. (1988). Proteolytic processing of
2 the alpha-chain of the lysosomal enzyme, beta-hexosaminidase, in normal human
3 fibroblasts. *J Biol Chem* **263**, 4288-92.
- 4 Maegawa, G. H., Stockley, T., Tropak, M., Banwell, B., Blaser, S., Kok, F., *et al.* (2006a). The natural
5 history of juvenile or subacute GM2 gangliosidosis: 21 new cases and literature review of 134
6 previously reported. *Pediatrics* **118**, e1550-62.
- 7 Maegawa, G. H., Tropak, M., Buttner, J., Stockley, T., Kok, F., Clarke, J. T., *et al.* (2007).
8 Pyrimethamine as a potential pharmacological chaperone for late-onset forms of GM2
9 gangliosidosis. *The Journal of biological chemistry* **282**, 9150-9161.
- 10 Maegawa, G. H. B., Stockley, T., Tropak, M., Banwell, B., Blaser, S., Kok, F., *et al.* (2006b). The
11 natural history of juvenile or subacute GM2 gangliosidosis: 21 new cases and literature
12 review of 134 previously reported. *Pediatrics* **118**, e1550-e1562.
- 13 Maiti, R., Van Domselaar, G. H., Zhang, H. & Wishart, D. S. (2004). SuperPose: a simple server for
14 sophisticated structural superposition. *Nucleic Acids Res* **32**, W590-4.
- 15 Mark, B. L., Mahuran, D. J., Cherney, M. M., Zhao, D., Knapp, S. & James, M. N. (2003). Crystal
16 structure of human beta-hexosaminidase B: understanding the molecular basis of Sandhoff
17 and Tay-Sachs disease. *J Mol Biol* **327**, 1093-109.
- 18 Mark, B. L., Vocadlo, D. J., Knapp, S., Triggs-Raine, B. L., Withers, S. G. & James, M. N. (2001).
19 Crystallographic evidence for substrate-assisted catalysis in a bacterial β -hexosaminidase.
20 *The Journal of biological chemistry* **276**, 10330-10337.
- 21 Masingue, M., Dufour, L., Lenglet, T., Saleille, L., Goizet, C., Ayrignac, X., *et al.* (2020). Natural
22 History of Adult Patients with GM2 Gangliosidosis. *Annals of neurology*, 10.1002/ana.25689.
- 23 Matsuzawa, F., Aikawa, S., Sakuraba, H., Lan, H. T., Tanaka, A., Ohno, K., *et al.* (2003). Structural
24 basis of the GM2 gangliosidosis B variant. *J Hum Genet* **48**, 582-9.
- 25 McCorvie, T. J. Timson, D. J. (2013). *In silico* prediction of the effects of mutations in the human UDP-
26 galactose 4'-epimerase gene: Towards a predictive framework for type III galactosemia.
27 *Gene* **524**, 95-104.
- 28 Mintseris, J. Weng, Z. (2005). Structure, function, and evolution of transient and obligate protein-
29 protein interactions. *Proc Natl Acad Sci U S A* **102**, 10930-5.
- 30 Mistri, M., Tamhankar, P. M., Sheth, F., Sanghavi, D., Kondurkar, P., Patil, S., *et al.* (2012).
31 Identification of novel mutations in HEXA gene in children affected with Tay Sachs disease
32 from India. *PLoS One* **7**, e39122.
- 33 Montalvo, A. L., Filocamo, M., Vlahovicek, K., Dardis, A., Lualdi, S., Corsolini, F., *et al.* (2005).
34 Molecular analysis of the HEXA gene in Italian patients with infantile and late onset Tay-
35 Sachs disease: detection of fourteen novel alleles. *Hum Mutat* **26**, 282.
- 36 Mules, E. H., Hayflick, S., Miller, C. S., Reynolds, L. W. & Thomas, G. H. (1992). Six novel deleterious
37 and three neutral mutations in the gene encoding the alpha-subunit of hexosaminidase A in
38 non-Jewish individuals. *Am J Hum Genet* **50**, 834-41.
- 39 Najmabadi, H., Hu, H., Garshasbi, M., Zemojtel, T., Abedini, S. S., Chen, W., *et al.* (2011). Deep
40 sequencing reveals 50 novel genes for recessive cognitive disorders. *Nature* **478**, 57-63.
- 41 Nakano, T., Muscillo, M., Ohno, K., Hoffman, A. J. & Suzuki, K. (1988). A point mutation in the coding
42 sequence of the beta-hexosaminidase alpha gene results in defective processing of the
43 enzyme protein in an unusual GM2-gangliosidosis variant. *J Neurochem* **51**, 984-7.
- 44 Nakano, T., Nanba, E., Tanaka, A., Ohno, K., Suzuki, Y. & Suzuki, K. (1990). A new point mutation
45 within exon 5 of beta-hexosaminidase alpha gene in a Japanese infant with Tay-Sachs
46 disease. *Ann Neurol* **27**, 465-73.

- 1 Navon, R., Khosravi, R., Korczyn, T., Masson, M., Sonnino, S., Fardeau, M., *et al.* (1995). A new
2 mutation in the HEXA gene associated with a spinal muscular atrophy phenotype. *Neurology*
3 **45**, 539-43.
- 4 Navon, R., Proia, R. L. (1989). The mutations in Ashkenazi Jews with adult GM2 gangliosidosis, the
5 adult form of Tay-Sachs disease. *Science* **243**, 1471-4.
- 6 Neote, K., Bapat, B., Dumbrille-Ross, A., Troxel, C., Schuster, S. M., Mahuran, D. J., *et al.* (1988).
7 Characterization of the human HEXB gene encoding lysosomal β -hexosaminidase. *Genomics*
8 **3**, 279-286.
- 9 Neudorfer, O., Pastores, G. M., Zeng, B. J., Gianutsos, J., Zaroff, C. M. & Kolodny, E. H. (2005). Late-
10 onset Tay-Sachs disease: phenotypic characterization and genotypic correlations in 21
11 affected patients. *Genet Med* **7**, 119-23.
- 12 Ohkuma, S., Poole, B. (1978). Fluorescence probe measurement of the intralysosomal pH in living
13 cells and the perturbation of pH by various agents. *Proc Natl Acad Sci U S A* **75**, 3327-31.
- 14 Ohno, K., Saito, S., Sugawara, K. & Sakuraba, H. (2008). Structural consequences of amino acid
15 substitutions causing Tay-Sachs disease. *Mol Genet Metab* **94**, 462-8.
- 16 Oliver, C., Timson, D. J. (2017). *In silico* prediction of the effects of mutations in the human triose
17 phosphate isomerase gene: Towards a predictive framework for TPI deficiency. *Eur J Med*
18 *Genet* **60**, 289-298.
- 19 Ornaghi, F., Sala, D., Tedeschi, F., Maffia, M. C., Bazzucchi, M., Morena, F., *et al.* (2020). Novel
20 bicistronic lentiviral vectors correct β -Hexosaminidase deficiency in neural and
21 hematopoietic stem cells and progeny: implications for in vivo and ex vivo gene therapy of
22 GM2 gangliosidosis. *Neurobiology of disease* **134**, 104667-104667.
- 23 Ou, L., Kim, S., Whitley, C. B. & Jarnes-Utz, J. R. (2019). Genotype-phenotype correlation of
24 gangliosidosis mutations using in silico tools and homology modeling. *Mol Genet Metab Rep*
25 **20**, 100495.
- 26 Ou, L., Przybilla, M. J., Tăbăran, A.-F., Overn, P., O'Sullivan, M. G., Jiang, X., *et al.* (2020). A novel
27 gene editing system to treat both Tay-Sachs and Sandhoff diseases. *Gene therapy*,
28 10.1038/s41434-019-0120-5.
- 29 Pandurangan, A. P., Ochoa-Montano, B., Ascher, D. B. & Blundell, T. L. (2017). SDM: a server for
30 predicting effects of mutations on protein stability. *Nucleic Acids Res* **45**, W229-W235.
- 31 Parthiban, V., Gromiha, M. M. & Schomburg, D. (2006). CUPSAT: prediction of protein stability upon
32 point mutations. *Nucleic Acids Res* **34**, W239-42.
- 33 Passos, O., Fernandes, P. A. & Ramos, M. J. (2011). QM/MM study of the catalytic mechanism of
34 GalNAc removal from GM2 ganglioside catalyzed by human β -hexosaminidase A. *The journal*
35 *of physical chemistry. B* **115**, 14751-14759.
- 36 Paw, B. H., Moskowitz, S. M., Uhrhammer, N., Wright, N., Kaback, M. M. & Neufeld, E. F. (1990).
37 Juvenile GM2 gangliosidosis caused by substitution of histidine for arginine at position 499
38 or 504 of the alpha-subunit of beta-hexosaminidase. *J Biol Chem* **265**, 9452-7.
- 39 Petroulakis, E., Cao, Z., Clarke, J. T., Mahuran, D. J., Lee, G. & Triggs-Raine, B. (1998). W474C amino
40 acid substitution affects early processing of the alpha-subunit of beta-hexosaminidase A and
41 is associated with subacute G(M2) gangliosidosis. *Hum Mutat* **11**, 432-42.
- 42 Pires, D. E., Ascher, D. B. & Blundell, T. L. (2014). mCSM: predicting the effects of mutations in
43 proteins using graph-based signatures. *Bioinformatics* **30**, 335-42.
- 44 Platt, F. M., Jeyakumar, M., Andersson, U., Priestman, D. A., Dwek, R. A., Butters, T. D., *et al.* (2001).
45 Inhibition of substrate synthesis as a strategy for glycolipid lysosomal storage disease
46 therapy. *Journal of inherited metabolic disease* **24**, 275-290.

- 1 Proia, R. L. Neufeld, E. F. (1982). Synthesis of beta-hexosaminidase in cell-free translation and in
2 intact fibroblasts: an insoluble precursor alpha chain in a rare form of Tay-Sachs disease.
3 *Proc Natl Acad Sci U S A* **79**, 6360-4.
- 4 Pundir, S., Martin, M. J. & O'Donovan, C. (2017). UniProt Protein Knowledgebase. *Methods Mol Biol*
5 **1558**, 41-55.
- 6 R-Project (2018). grep - Pattern Matching And Replacement.
- 7 Raghavan, S. S., Krusell, A., Krusell, J., Lyerla, T. A. & Kolodny, E. H. (1985). GM2-ganglioside
8 metabolism in hexosaminidase A deficiency states: determination in situ using labeled GM2
9 added to fibroblast cultures. *Am J Hum Genet* **37**, 1071-82.
- 10 Ribeiro, M. G., Sonin, T., Pinto, R. A., Fontes, A., Ribeiro, H., Pinto, E., *et al.* (1996). Clinical,
11 enzymatic, and molecular characterisation of a Portuguese family with a chronic form of
12 GM2-gangliosidosis B1 variant. *J Med Genet* **33**, 341-3.
- 13 Robinson, D. Stirling, J. L. (1968). N-Acetyl- β -glucosaminidases in human spleen. *The Biochemical*
14 *journal* **107**, 321-327.
- 15 Rountree, J. S., Butters, T. D., Wormald, M. R., Boomkamp, S. D., Dwek, R. A., Asano, N., *et al.*
16 (2009). Design, synthesis, and biological evaluation of enantiomeric β -N-
17 acetylhexosaminidase inhibitors LABNAc and DABNAc as potential agents against Tay-
18 Sachs and Sandhoff disease. *ChemMedChem* **4**, 378-392.
- 19 Schrödinger, L. (2018). The PyMOL Molecular Graphics System, Version 2.0
- 20 Shapiro, B. E. Natowicz, M. R. (2009). Late-onset Tay-Sachs disease presenting as a childhood
21 stutter. *J Neurol Neurosurg Psychiatry* **80**, 94-5.
- 22 Sharma, R., Bukovac, S., Callahan, J. & Mahuran, D. (2003a). A single site in human beta-
23 hexosaminidase A binds both 6-sulfate-groups on hexosamines and the sialic acid moiety of
24 GM2 ganglioside. *Biochim Biophys Acta* **1637**, 113-8.
- 25 Sharma, R., Bukovac, S., Callahan, J. & Mahuran, D. (2003b). A single site in human β -
26 hexosaminidase A binds both 6-sulfate-groups on hexosamines and the sialic acid moiety of
27 GM2 ganglioside. *Biochimica et biophysica acta* **1637**, 113-118.
- 28 Sheth, J., Mistri, M., Sheth, F., Shah, R., Bavdekar, A., Godbole, K., *et al.* (2014). Burden of lysosomal
29 storage disorders in India: experience of 387 affected children from a single diagnostic
30 facility. *JIMD Rep* **12**, 51-63.
- 31 Sievers, F., Wilm, A., Dineen, D., Gibson, T. J., Karplus, K., Li, W., *et al.* (2011). Fast, scalable
32 generation of high-quality protein multiple sequence alignments using Clustal Omega. *Mol*
33 *Syst Biol* **7**, 539.
- 34 Sormanni, P., Aprile, F. A. & Vendruscolo, M. (2015). The CamSol method of rational design of
35 protein mutants with enhanced solubility. *J Mol Biol* **427**, 478-90.
- 36 Specola, N., Vanier, M. T., Goutieres, F., Mikol, J. & Aicardi, J. (1990). The juvenile and chronic forms
37 of GM2 gangliosidosis: clinical and enzymatic heterogeneity. *Neurology* **40**, 145-50.
- 38 Steiner, K. M., Brenck, J., Goericke, S. & Timmann, D. (2016). Cerebellar atrophy and muscle
39 weakness: late-onset Tay-Sachs disease outside Jewish populations. *BMJ Case Rep* **2016**.
- 40 Svennerholm, L. Fredman, P. (1980). A procedure for the quantitative isolation of brain gangliosides.
41 *Biochim Biophys Acta* **617**, 97-109.
- 42 Tabeta, K., Hoebe, K., Janssen, E. M., Du, X., Georgel, P., Crozat, K., *et al.* (2006). The Unc93b1
43 mutation 3d disrupts exogenous antigen presentation and signaling via Toll-like receptors 3,
44 7 and 9. *Nat Immunol* **7**, 156-64.
- 45 Tanaka, A., Hoang, L. T., Nishi, Y., Maniwa, S., Oka, M. & Yamano, T. (2003a). Different attenuated
46 phenotypes of GM2 gangliosidosis variant B in Japanese patients with HEXA mutations at

codon 499, and five novel mutations responsible for infantile acute form. *J Hum Genet* **48**, 571-4.

- 1
2
3
4
5
6
7
8
9
10
11
12
13
14
15
16
17
18
19
20
21
22
23
24
25
26
27
28
29
30
31
32
33
34
35
36
37
38
39
40
41
42
43
44
45
46
47
48
49
50
51
52
53
54
55
56
57
58
59
60
61
62
63
64
65
- Tanaka, A., Hoang, L. T. N., Nishi, Y., Maniwa, S., Oka, M. & Yamano, T. (2003b). Different attenuated phenotypes of GM2 gangliosidosis variant B in Japanese patients with HEXA mutations at codon 499, and five novel mutations responsible for infantile acute form. *Journal of human genetics* **48**, 571-574.
- Tanaka, A., Ohno, K., Sandhoff, K., Maire, I., Kolodny, E. H., Brown, A., *et al.* (1990a). GM2-gangliosidosis B₁ variant: analysis of beta-hexosaminidase alpha gene abnormalities in seven patients. *Am J Hum Genet* **46**, 329-39.
- Tanaka, A., Punnett, H. H. & Suzuki, K. (1990b). A new point mutation in the beta-hexosaminidase alpha subunit gene responsible for infantile Tay-Sachs disease in a non-Jewish Caucasian patient (a Kpn mutant). *Am J Hum Genet* **47**, 568-74.
- Tanaka, A., Sakazaki, H., Murakami, H., Isshiki, G. & Suzuki, K. (1994). Molecular genetics of Tay-Sachs disease in Japan. *J Inherit Metab Dis* **17**, 593-600.
- Tartaglia, G. G. & Vendruscolo, M. (2008). The Zyggregator method for predicting protein aggregation propensities. *Chem Soc Rev* **37**, 1395-401.
- Team,, L. (2018). Lazarus v1.82: The professional Free Pascal RAD IDE.
- Team,, R. (2016). RStudio: Integrated Development Environment for R.
- Tettamanti, G. (2004). Ganglioside/glycosphingolipid turnover: new concepts. *Glycoconj J* **20**, 301-17.
- Timson, D. J. (2015). Value of predictive bioinformatics in inherited metabolic diseases. *World Journal of Medical Genetics* **5**, 46-51.
- Triggs-Raine, B. L., Akerman, B. R., Clarke, J. T. & Gravel, R. A. (1991). Sequence of DNA flanking the exons of the HEXA gene, and identification of mutations in Tay-Sachs disease. *Am J Hum Genet* **49**, 1041-54.
- Trop, I., Kaplan, F., Brown, C., Mahuran, D. & Hechtman, P. (1992). A glycine250--> aspartate substitution in the alpha-subunit of hexosaminidase A causes juvenile-onset Tay-Sachs disease in a Lebanese-Canadian family. *Hum Mutat* **1**, 35-9.
- Tropak, M. B., Bukovac, S. W., Rigat, B. A., Yonekawa, S., Wakarchuk, W. & Mahuran, D. J. (2010). A sensitive fluorescence-based assay for monitoring GM2 ganglioside hydrolysis in live patient cells and their lysates. *Glycobiology* **20**, 356-365.
- Tropak, M. B., Reid, S. P., Guiral, M., Withers, S. G. & Mahuran, D. (2004). Pharmacological enhancement of β -hexosaminidase activity in fibroblasts from adult Tay-Sachs and Sandhoff Patients. *The Journal of biological chemistry* **279**, 13478-13487.
- Tsuji, D., Akeboshi, H., Matsuoka, K., Yasuoka, H., Miyasaki, E., Kasahara, Y., *et al.* (2011). Highly phosphomannosylated enzyme replacement therapy for GM2 gangliosidosis. *Annals of Neurology* **69**, 691-701.
- UniProt Consortium, T. (2018). UniProt: the universal protein knowledgebase. *Nucleic Acids Res* **46**, 2699.
- Valdar, W. S. (2002). Scoring residue conservation. *Proteins* **48**, 227-241.
- Valdar, W. S. & Thornton, J. M. (2001). Conservation helps to identify biologically relevant crystal contacts. *J Mol Biol* **313**, 399-416.
- Zampieri, S., Montalvo, A., Blanco, M., Zanin, I., Amartino, H., Vlahovicek, K., *et al.* (2012). Molecular analysis of HEXA gene in Argentinean patients affected with Tay-Sachs disease: possible common origin of the prevalent c.459+5A>G mutation. *Gene* **499**, 262-5.

Table

Table 1: The variants included in this study, their phenotype and references to the studies describing them.

Variant	TSD Variant	Reference	Provean Score	SIFT Score
Leu39Arg	Infantile	(Akli <i>et al.</i> , 1993b)	-4.49 (Deleterious)	0.001 (Damaging)
Glu114Lys	Infantile	(Mistri <i>et al.</i> , 2012) (Sheth <i>et al.</i> , 2014)	-3.68 (Deleterious)	0.001 (Damaging)
Leu127Arg	Infantile	(Akli <i>et al.</i> , 1993b; Montalvo <i>et al.</i> , 2005)	-5.48 (Deleterious)	0.000 (Damaging)
Arg170Gln	Infantile	(Drucker <i>et al.</i> , 1992; Kaufman <i>et al.</i> , 1997; Nakano <i>et al.</i> , 1990)	-3.85 (Deleterious)	0.000 (Damaging)
Arg170Trp	Infantile	(Mistri <i>et al.</i> , 2012; Sheth <i>et al.</i> , 2014; Triggs-Raine <i>et al.</i> , 1991)	-7.71 (Deleterious)	0.000 (Damaging)
Arg178Cys	B1 (Infantile)	(Navon <i>et al.</i> , 1995; Tanaka <i>et al.</i> , 1990a)	-7.71 (Deleterious)	0.000 (Damaging)
Arg178Leu	B1 (Infantile)	(Triggs-Raine <i>et al.</i> , 1991)	-6.74 (Deleterious)	0.000 (Damaging)
Val192Leu	Infantile	(Ainsworth & Coulter-Mackie, 1992; Hou <i>et al.</i> , 1996)	-1.26 (Neutral)	0.002 (Damaging)
His204Arg	Infantile	(Akli <i>et al.</i> , 1993b)	-7.8 (Deleterious)	0.000 (Damaging)
Ser210Phe	Infantile	(Akli <i>et al.</i> , 1991)	-5.82 (Deleterious)	0.000 (Damaging)

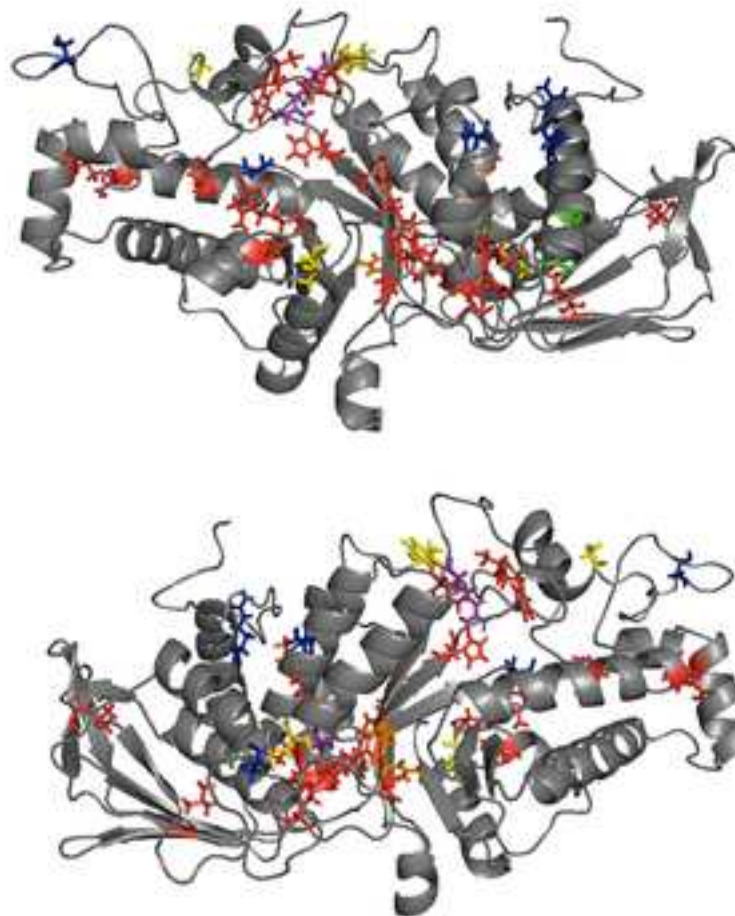
Phe211Ser	Infantile	(Akli <i>et al.</i> , 1993b; Brown <i>et al.</i> , 1989; Montalvo <i>et al.</i> , 2005)	-7.73 (Deleterious)	0.000 (Damaging)
Arg252Leu	Infantile	(Tanaka <i>et al.</i> , 2003a)	-6.83 (Deleterious)	0.002 (Damaging)
Asn295Ser	Infantile	(Tanaka <i>et al.</i> , 2003a)	-4.19 (Deleterious)	0.05 (Damaging)
Met301Arg	Infantile	(Akli <i>et al.</i> , 1993b)	-4.87 (Deleterious)	0.001 (Damaging)
Asp322Asn	Infantile	(Mistri <i>et al.</i> , 2012) (Sheth <i>et al.</i> , 2014)	-4.88 (Deleterious)	0.000 (Damaging)
Asp322Tyr	Infantile	(Mistri <i>et al.</i> , 2012; Sheth <i>et al.</i> , 2014)	-8.73 (Deleterious)	0.000 (Damaging)
Gln374Arg	Infantile	(Montalvo <i>et al.</i> , 2005)	-3.92 (Deleterious)	0.001 (Damaging)
Gln374Pro	Infantile	(Sheth <i>et al.</i> , 2014)	-5.88 (Deleterious)	0.001 (Damaging)
Arg393Pro	Infantile	(Mistri <i>et al.</i> , 2012; Sheth <i>et al.</i> , 2014)	-2.57 (Deleterious)	0.005 (Damaging)
Trp420Cys	Infantile	(Matsuzawa <i>et al.</i> , 2003; Tanaka <i>et al.</i> , 2003a; Tanaka <i>et al.</i> , 1990b)	-12.44 (Deleterious)	0.000 (Damaging)
Cys458Tyr	Infantile	(Matsuzawa <i>et al.</i> , 2003; Tanaka <i>et al.</i> , 1994)	-9.5 (Deleterious)	0.000 (Damaging)
Glu462Val	Infantile	(Mistri <i>et al.</i> , 2012; Sheth <i>et al.</i> , 2014)	-6.62 (Deleterious)	0.000 (Damaging)
Gly478Arg	Infantile	(Mistri <i>et al.</i> , 2012; Sheth <i>et al.</i> , 2014)	-2.16 (Neutral)	0.012 (Damaging)

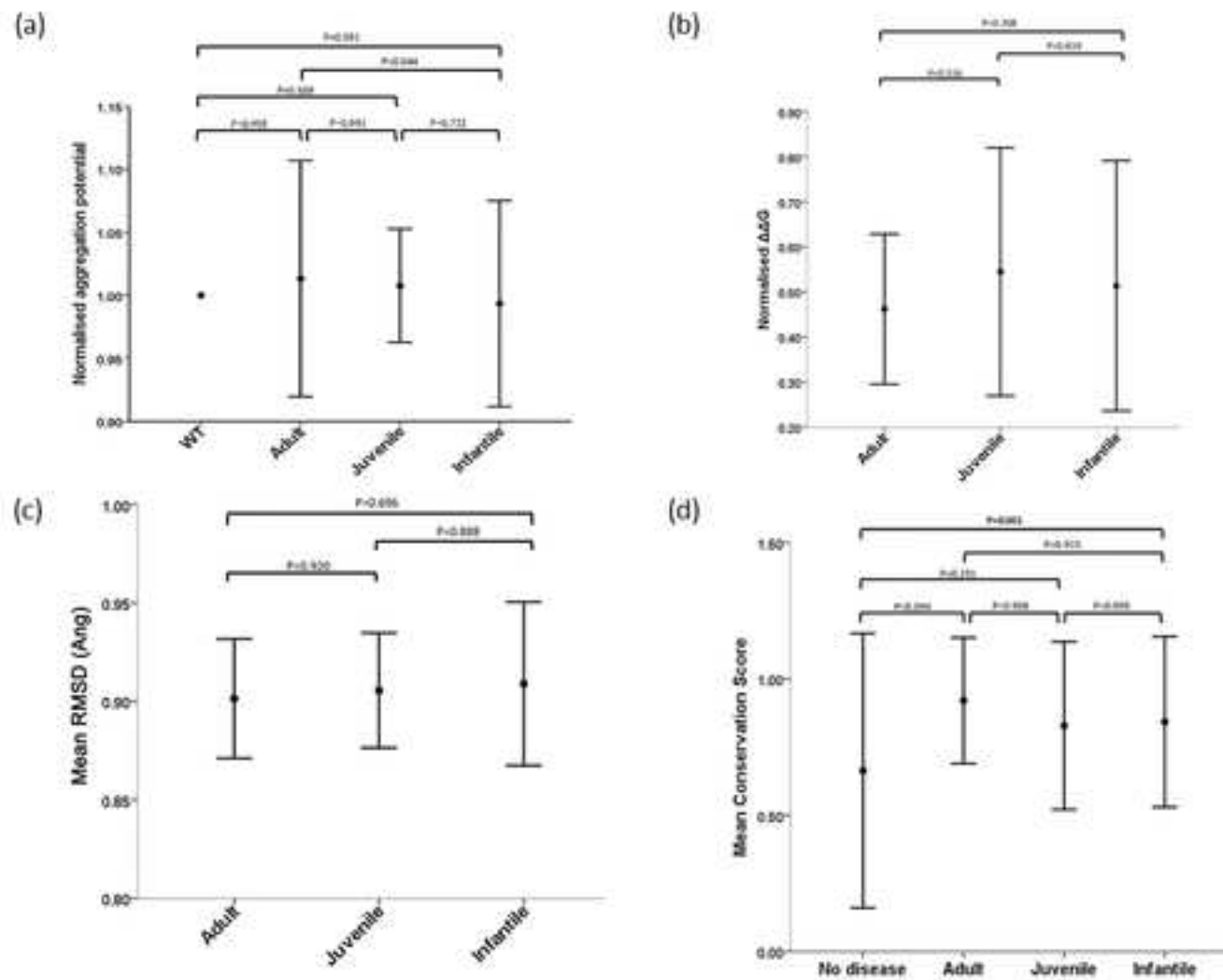
Glu482Lys	Infantile	(Dersh <i>et al.</i> , 2016; Nakano <i>et al.</i> , 1988; Proia & Neufeld, 1982)	-3.71 (Deleterious)	0.000 (Damaging)
Leu484Gln	Infantile	(Tanaka <i>et al.</i> , 1994)	-5.57 (Deleterious)	0.000 (Damaging)
Leu484Pro	Infantile	(Tanaka <i>et al.</i> , 1994)	-6.5 (Deleterious)	0.000 (Damaging)
Arg504Cys	Infantile	(Akli <i>et al.</i> , 1991; Boonyawat, 2016; Montalvo <i>et al.</i> , 2005; Neudorfer <i>et al.</i> , 2005; Paw <i>et al.</i> , 1990; Raghavan <i>et al.</i> , 1985; Shapiro & Natowicz, 2009)	-7.43 (Deleterious)	0.003 (Damaging)
Trp485Arg	Infantile	(Akalin <i>et al.</i> , 1992)	-13 (Deleterious)	0.000 (Damaging)
Cys58Tyr	Juvenile	(Najmabadi <i>et al.</i> , 2011)	-8.58 (Deleterious)	0.001 (Damaging)
Arg178His	B1 (Juvenile)	(Brown <i>et al.</i> , 1989; Giraud <i>et al.</i> , 2010; Maegawa <i>et al.</i> , 2006a; Montalvo <i>et al.</i> , 2005; Ou <i>et al.</i> , 2019; Tanaka <i>et al.</i> , 1990a)	-4.82 (Deleterious)	0.000 (Damaging)
Gly250Asp	Juvenile	(Trop <i>et al.</i> , 1992)	-6.83 (Deleterious)	0.001 (Damaging)
Asp258His	B1 (Juvenile)	(Fernandes <i>et al.</i> , 1992; Fernandes <i>et al.</i> , 1997)	-6.83 (Deleterious)	0.000 (Damaging)
Ser279Pro	Juvenile	(Drucker <i>et al.</i> , 1997)	-2.89 (Deleterious)	0.06 (Tolerated)
Trp474Cys	Juvenile	(Maegawa <i>et al.</i> , 2006a; Neudorfer <i>et al.</i> , 2005; Petroulakis <i>et al.</i> , 1998)	-12.21 (Deleterious)	0.000 (Damaging)

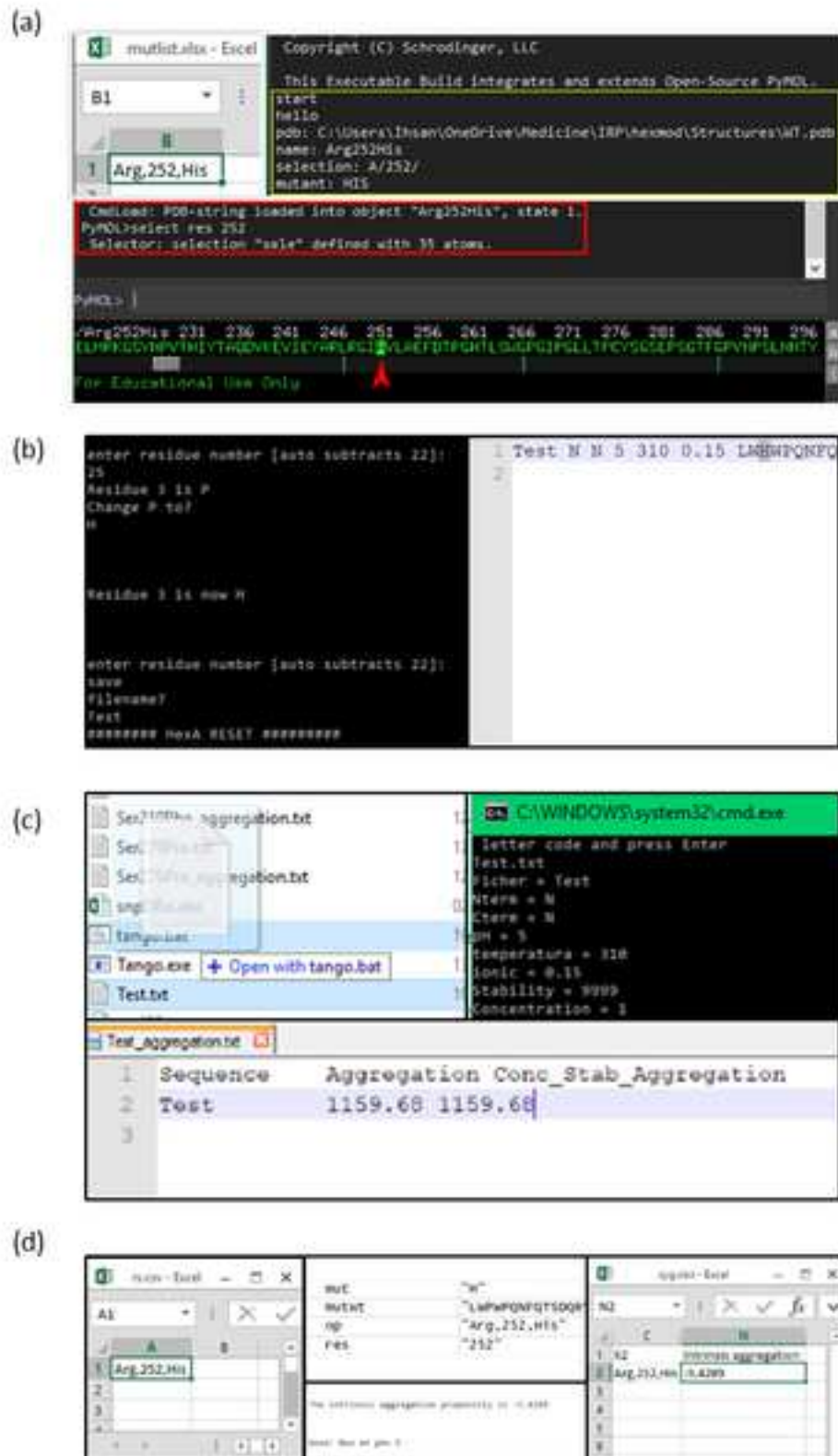
1	Arg499His	Juvenile	(Maegawa <i>et al.</i> , 2006a; Ou <i>et al.</i> , 2019; Paw <i>et al.</i> , 1990; Shapiro & Natowicz, 2009; Tanaka <i>et al.</i> , 2003a; Zampieri <i>et al.</i> , 2012)	-4.64 (Deleterious)	0.000 (Damaging)
2					
3					
4					
5					
6					
7					
8					
9	Arg499Cys	Juvenile	(Akli <i>et al.</i> , 1993a; Mules <i>et al.</i> , 1992; Tanaka <i>et al.</i> , 2003b)	-7.43 (Deleterious)	0.000 (Damaging)
10					
11					
12					
13					
14					
15	Arg504His	Juvenile	(Giraud <i>et al.</i> , 2010; Paw <i>et al.</i> , 1990)	-4.64 (Deleterious)	0.001 (Damaging)
16					
17					
18					
19					
20	Tyr180His	Adult	(De Gasperi <i>et al.</i> , 1996)	-4.45 (Deleterious)	0.000 (Damaging)
21					
22					
23					
24	Lys197Thr	Adult	(Akli <i>et al.</i> , 1993b)	-5.85 (Deleterious)	0.000 (Damaging)
25					
26					
27	Arg252His	Adult	(Ribeiro <i>et al.</i> , 1996)	-4.88 (Deleterious)	0.001 (Damaging)
28					
29					
30	Gly269Ser	Adult	(Maegawa <i>et al.</i> , 2006a; Navon & Proia, 1989; Neudorfer <i>et al.</i> , 2005; Shapiro & Natowicz, 2009)	-5.51 (Deleterious)	0.177 (Tolerated)
31					
32					
33					
34					
35					
36					
37					
38	Val391Met	Adult	(Navon <i>et al.</i> , 1995)	-2.79 (Deleterious)	0.001 (Damaging)
39					
40					
41					



(b)







Supplementary dataSupplementary Table S1 Identifiers of HexA sequences used in alignment

XP_003413972.1 beta-hexosaminidase subunit alpha isoform X2 [*Loxodonta africana*]
XP_023408658.1 beta-hexosaminidase subunit alpha isoform X1 [*Loxodonta africana*]
XP_023408659.1 beta-hexosaminidase subunit alpha isoform X3 [*Loxodonta africana*]
XP_020018929.1 beta-hexosaminidase subunit alpha [*Castor canadensis*]
NP_001133930.1 beta-hexosaminidase subunit beta [*Salmo salar*]
XP_011395527.1 Beta-hexosaminidase subunit alpha [*Auxenochlorella protothecoides*]
XP_022435662.1 beta-hexosaminidase subunit alpha isoform X1 [*Delphinapterus leucas*]
XP_022435663.1 beta-hexosaminidase subunit alpha isoform X2 [*Delphinapterus leucas*]
XP_022435664.1 beta-hexosaminidase subunit alpha isoform X3 [*Delphinapterus leucas*]
XP_021409901.1 beta-hexosaminidase subunit alpha [*Lonchura striata domestica*]
XP_020659346.1 beta-hexosaminidase subunit alpha [*Pogona vitticeps*]
XP_010410730.2 beta-hexosaminidase subunit alpha [*Corvus cornix cornix*]
XP_004628811.1 beta-hexosaminidase subunit alpha isoform X1 [*Octodon degus*]
XP_023568375.1 beta-hexosaminidase subunit alpha isoform X2 [*Octodon degus*]
XP_544758.2 beta-hexosaminidase subunit alpha isoform X1 [*Canis lupus familiaris*]
XP_013965054.1 beta-hexosaminidase subunit alpha isoform X2 [*Canis lupus familiaris*]
XP_022268255.1 beta-hexosaminidase subunit alpha isoform X3 [*Canis lupus familiaris*]
XP_019687278.1 beta-hexosaminidase subunit alpha isoform X1 [*Felis catus*]
XP_012996870.1 beta-hexosaminidase subunit alpha [*Cavia porcellus*]
XP_022367876.1 beta-hexosaminidase subunit alpha [*Enhydra lutris kenyoni*]
XP_005069690.1 beta-hexosaminidase subunit alpha isoform X2 [*Mesocricetus auratus*]
XP_012968476.1 beta-hexosaminidase subunit alpha isoform X1 [*Mesocricetus auratus*]
XP_012968477.1 beta-hexosaminidase subunit alpha isoform X3 [*Mesocricetus auratus*]
XP_012623694.1 beta-hexosaminidase subunit alpha isoform X1 [*Microcebus murinus*]
XP_012623695.1 beta-hexosaminidase subunit alpha isoform X2 [*Microcebus murinus*]
XP_020784475.1 beta-hexosaminidase subunit alpha [*Boleophthalmus pectinirostris*]
XP_022610337.1 beta-hexosaminidase subunit alpha [*Seriola dumerili*]
XP_021549757.1 beta-hexosaminidase subunit alpha isoform X1 [*Neomonachus schauinslandi*]
XP_021549758.1 beta-hexosaminidase subunit alpha isoform X2 [*Neomonachus schauinslandi*]

XP_021262712.1 beta-hexosaminidase subunit alpha [*Numida meleagris*]
XP_001494361.1 beta-hexosaminidase subunit alpha [*Equus caballus*]
XP_004070040.1 beta-hexosaminidase subunit alpha isoform X1 [*Oryzias latipes*]
XP_020559701.1 beta-hexosaminidase subunit alpha isoform X2 [*Oryzias latipes*]
XP_020852539.1 beta-hexosaminidase subunit alpha isoform X1 [*Phascolarctos cinereus*]
XP_020852541.1 beta-hexosaminidase subunit alpha isoform X2 [*Phascolarctos cinereus*]
XP_011373887.1 beta-hexosaminidase subunit alpha isoform X1 [*Pteropus vampyrus*]
XP_023377626.1 beta-hexosaminidase subunit alpha isoform X2 [*Pteropus vampyrus*]
XP_023377628.1 beta-hexosaminidase subunit alpha isoform X3 [*Pteropus vampyrus*]
XP_006087896.1 beta-hexosaminidase subunit alpha [*Myotis lucifugus*]
XP_012306688.1 beta-hexosaminidase subunit alpha isoform X1 [*Aotus nancymaae*]
XP_012306689.1 beta-hexosaminidase subunit alpha isoform X2 [*Aotus nancymaae*]
XP_012306690.1 beta-hexosaminidase subunit alpha isoform X3 [*Aotus nancymaae*]
XP_012306697.1 beta-hexosaminidase subunit alpha isoform X6 [*Aotus nancymaae*]
XP_021494470.1 beta-hexosaminidase subunit alpha [*Meriones unguiculatus*]
XP_021165578.1 beta-hexosaminidase subunit alpha [*Fundulus heteroclitus*]
XP_012931717.1 beta-hexosaminidase subunit alpha isoform X2 [*Heterocephalus glaber*]
XP_021092627.1 beta-hexosaminidase subunit alpha isoform X1 [*Heterocephalus glaber*]
XP_021092628.1 beta-hexosaminidase subunit alpha isoform X3 [*Heterocephalus glaber*]
XP_004463787.1 beta-hexosaminidase subunit alpha isoform X1 [*Dasypus novemcinctus*]
XP_004463788.1 beta-hexosaminidase subunit alpha isoform X2 [*Dasypus novemcinctus*]
XP_020749943.1 beta-hexosaminidase subunit alpha isoform X1 [*Odocoileus virginianus texanus*]
XP_020749946.1 beta-hexosaminidase subunit alpha isoform X2 [*Odocoileus virginianus texanus*]
XP_003901203.1 beta-hexosaminidase subunit alpha [*Papio anubis*]
XP_008071051.1 beta-hexosaminidase subunit alpha isoform X1 [*Carlito syrincta*]
XP_021561799.1 beta-hexosaminidase subunit alpha isoform X2 [*Carlito syrincta*]
XP_020953572.1 beta-hexosaminidase subunit alpha isoform X1 [*Sus scrofa*]
XP_021156454.1 beta-hexosaminidase subunit alpha [*Columba livia*]
XP_021027405.1 beta-hexosaminidase subunit alpha [*Mus caroli*]
XP_023278359.1 beta-hexosaminidase subunit alpha [*Seriola lalandi dorsalis*]
XP_021062583.1 beta-hexosaminidase subunit alpha [*Mus pahari*]
XP_003784529.1 beta-hexosaminidase subunit alpha [*Otolemur garnettii*]

XP_023205502.1 beta-hexosaminidase subunit alpha [*Xiphophorus maculatus*]
XP_022045995.1 beta-hexosaminidase subunit alpha [*Acanthochromis polyacanthus*]
XP_003755208.1 beta-hexosaminidase subunit alpha [*Sarcophilus harrisii*]
XP_005316823.1 beta-hexosaminidase subunit alpha isoform X1 [*Ictidomys tridecemlineatus*]
XP_021583780.1 beta-hexosaminidase subunit alpha isoform X2 [*Ictidomys tridecemlineatus*]
XP_004374779.1 beta-hexosaminidase subunit alpha isoform X1 [*Trichechus manatus latirostris*]
XP_023585564.1 beta-hexosaminidase subunit alpha isoform X2 [*Trichechus manatus latirostris*]
XP_003378067.1 beta-hexosaminidase subunit alpha [*Trichinella spiralis*]
XP_023076435.1 beta-hexosaminidase subunit alpha [*Piliocolobus tephrosceles*]
XP_004553154.1 beta-hexosaminidase subunit alpha isoform X1 [*Maylandia zebra*]
XP_023008256.1 beta-hexosaminidase subunit alpha isoform X2 [*Maylandia zebra*]
XP_021326163.1 beta-hexosaminidase subunit alpha isoform X1 [*Danio rerio*]